Received: 5 May 2020 | Revised: 18 July 2020 | Accepted: 21 July 2020

DOI: 10.1002/jimd.12291

ORIGINAL ARTICLE

JIMD SSIEM WILEY

Serum bikunin isoforms in congenital disorders of glycosylation and linkeropathies

Walid Haouari[1] | Johanne Dubail[2] | Samra Lounis-Ouaras[1,3] | Pierre Prada[4] | Rizk Bennani[4] | Charles Roseau[1] | Céline Huber[2] | Alexandra Afenjar[5] | Estelle Colin[6,7] | Sandrine Vuillaumier-Barrot[4] | Nathalie Seta[4,8] | François Foulquier[9] | Christian Poüs[1,3] | Valérie Cormier-Daire[2] | Arnaud Bruneel[1,4]

[1]INSERM UMR1193, Université Paris-Saclay, Châtenay-Malabry, France

[2]Department of Clinical Genetics and Reference Centre for Constitutional Bone Diseases, INSERM U1163, Université de Paris, Imagine Institute, Necker-Enfants Malades Hospital, AP-HP, Paris, France

[3]AP-HP, Biochimie-Hormonologie, Hôpital Antoine Béclère, Clamart, France

[4]AP-HP, Biochimie Métabolique et Cellulaire, Hôpital Bichat-Claude Bernard, Paris, France

[5]Département de Génétique et Embryologie Médicale, Sorbonne Universités, Centre de Référence Malformations et Maladies Congénitales du Cervelet et Déficiences Intellectuelles de Causes Rares, Hôpital Trousseau, AP-HP, Paris, France

[6]Department of Biochemistry and Genetics, University Hospital, Angers, France

[7]MitoLab Team, Institut MitoVasc, UMR CNRS6015, INSERM U1083, Angers, France

[8]Université de Paris, Paris, France

[9]Université de Lille, CNRS, UMR 8576 – UGSF - Unité de Glycobiologie Structurale et Fonctionnelle, Lille, France

Correspondence
Arnaud Bruneel, INSERM UMR1193, "Mécanismes Cellulaires et Moléculaires de l'Adaptation au Stress et Cancérogenèse," Faculté de Pharmacie de Chatenay-Malabry, Tour D4, 1er étage, 5 rue Jean Baptiste Clément, 92220 Chatenay-Malabry, France.
Email: arnaud.bruneel@aphp.fr

Communicating Editor: Ron A Wevers

Funding information
Agence Nationale de la Recherche, Grant/Award Number: 15RAR3-0004-06; European Union's Horizon 2020 Research and Innovation Program, Grant/Award Number: 643578

Abstract

Bikunin (Bkn) isoforms are serum chondroitin sulfate (CS) proteoglycans synthesized by the liver. They include two light forms, that is, the Bkn core protein and the Bkn linked to the CS chain (urinary trypsin inhibitor [UTI]), and two heavy forms, that is, pro-α-trypsin inhibitor and inter-α-trypsin inhibitor, corresponding to UTI esterified by one or two heavy chains glycoproteins, respectively. We previously showed that the Western-blot analysis of the light forms could allow the fast and easy detection of patients with linkeropathy, deficient in enzymes involved in the synthesis of the initial common tetrasaccharide linker of glycosaminoglycans. Here, we analyzed all serum Bkn isoforms in a context of congenital disorders of glycosylation (CDG) and showed very specific abnormal patterns suggesting potential interests for their screening and diagnosis. In particular, genetic deficiencies in V-ATPase

Abbreviations: Alb, albumin; ALP, alkaline phosphatase; ApoC-III, apolipoprotein C-III; B3GALT6, beta-1,3-galactosyltransferase 6; B3GAT3, beta-1,3-glucuronyltransferase 3; B4GALT7, beta-1,4-galactosyltransferase 7; Bkn, bikunin; Bkn-CS, bikunin linked to chondroitin sulfate chain; CDG, congenital disorder(s) of glycosylation; COG, conserved oligomeric Golgi complex; CS, chondroitin sulfate; ER, endoplasmic reticulum; GAG, glycosaminoglycan; Gal, galactose; GlcA, glucuronic acid; GlcNAc, *N*-acetylglucosamine; HC, heavy chain protein; ITI, inter-α-trypsin inhibitor; Mn^{2+}, manganese; PG, proteoglycans; PTMs, posttranslational modifications; PαI, pro-α-trypsin inhibitor; SLC35A2, solute carrier family 35 member A2; SLC35A3, solute carrier family 35 member A3; TBS, Tris buffer saline; TMEM165, transmembrane protein 165; Trf, transferrin; TTBS, TBS with 0.1% Tween; UTI, urinary trypsin inhibitor; Xyl, xylose.

(ATP6V0A2-CDG, CCDC115-CDG, ATP6AP1-CDG), in Golgi manganese homeostasis (TMEM165-CDG) and in the *N*-acetyl-glucosamine Golgi transport (SLC35A3-CDG) all share specific abnormal Bkn patterns. Furthermore, for each studied linkeropathy, we show that the light abnormal Bkn could be further in-depth characterized by two-dimensional electrophoresis. Moreover, besides being interesting as a specific biomarker of both CDG and linkeropathies, Bkn isoforms' analyses can provide new insights into the pathophysiology of the aforementioned diseases.

KEYWORDS

bikunin, CDG, GAG tetrasaccharide, inter-α-trypsin inhibitor, linkeropathies, SLC35A3, TMEM165

1 | INTRODUCTION

Bikunin (Bkn) isoforms are serum proteoglycans of liver origin bearing a chondroitin sulfate (CS) chain mainly esterified by one or two glycoproteins named "heavy chains" (HCs). Three major serum isoforms have been extensively described: the inter-α-trypsin inhibitor (ITI) and the pro-α-trypsin inhibitor (PαI), carrying respectively two and one HC, as well as the urinary trypsin inhibitor (UTI), which corresponds to Bkn linked to the CS chain.[1] In addition, we showed that free Bkn (ie, the core protein) could be detected at low level in serum[2] (Figure 1A).

UTI (Bkn-CS) results from the linkage of one xylose (Xyl) residue to the Ser10 of Bkn followed by the sequential action of enzymes catalyzing the biosynthesis of the PG common tetrasaccharide linker (GlcA-Gal-Gal-Xyl-O-Ser) and the elongation of a short CS chain consisting of 15 ± 3 (GlcA-GalNAc) sulfated disaccharide motifs. The tetrasaccharide linker synthesis starts in the endoplasmic reticulum (ER) lumen while the elongation occurs in the Golgi compartment. This requires specific glycoenzymes, nucleotide sugars, and an activated form of sulfate as substrates.[3,4] Once the Bkn CS chain is elongated and sulfated, it covalently binds one or two HC(s) leading to PαI and ITI, respectively (heavy Bkn isoforms) (Figure 1B). Noticeably, the ester linkages between the HCs and the CS chain occur in the *trans*-Golgi after a pH-dependent C-terminal autocatalytic cleavage of HC proteins precursors.[5] Besides the linkage and the elongation of the CS chain, the core protein Bkn and HCs precursors are *N*-glycosylated, *O*-glycosylated and undergo proteolytic cleavage in the ER and the Golgi. Thus, with the reported CS chain phosphorylation, sulfation, and sialylation, a large range of posttranslational modifications (PTMs) can be found on serum Bkn isoforms[3,6-9] (Figure 1B).

In pathophysiology, under stimuli such as inflammation or ovulation, circulating ITI and PαI can be extravasated from the blood, playing an important role in the stabilization of the extracellular matrices through the exchange of HCs with hyaluronic acid.[10,11] Moreover, the Bkn core protein has been shown to inhibit inflammation-associated proteases such as trypsin, elastase, and plasmin in pancreatitis, septic shock and rheumatoid arthritis.[12,13] In some cancers, Bkn has been shown to inhibit cell proliferation, thus attenuating tumor invasion.[14] Finally, Bkn isoforms exert inhibitory activity toward calcium oxalate crystal formation and therefore has protective effects against kidney stones and urolithiasis.[15]

In linkeropathies, that is, rare skeletal/osteoarticular genetic diseases affecting the biosynthesis of the common initial tetrasaccharide (-GlcA-Gal-Gal-Xyl-O-Ser-) of protein-linked glycosaminoglycans (GAG), we previously showed high levels of abnormal serum Bkn light forms suggesting a potential interest for screening purposes.[2]

In this work, we performed Western-blot analysis of all serum Bkn isoforms from patients with various congenital disorders of glycosylation (CDG) including defects in the V-ATPase Golgi protons pump (ATP6V0A2-CDG, CCDC115-CDG, and ATP6AP1-CDG), in manganese (Mn^{2+}) homeostasis (TMEM165-CDG), in tethering factors (conserved oligomeric Golgi complex [COG]-CDG) and in activated sugar transporters (SLC35A2-CDG and SLC35A3-CDG). We focused on these CDG because we anticipated the presence of abnormal Bkn isoforms, linked to impaired Golgi homeostasis (V-ATPase deficiencies, TMEM165-CDG, COG-CDG), and/or associated with GAG biosynthesis defects leading to skeletal clinical phenotypes (TMEM165-CDG, SLC35A2-CDG, and SLC35A3-CDG). Furthermore, we carried out the characterization of abnormal Bkn light forms in linkeropathies by using two-dimensional electrophoresis (2-DE).

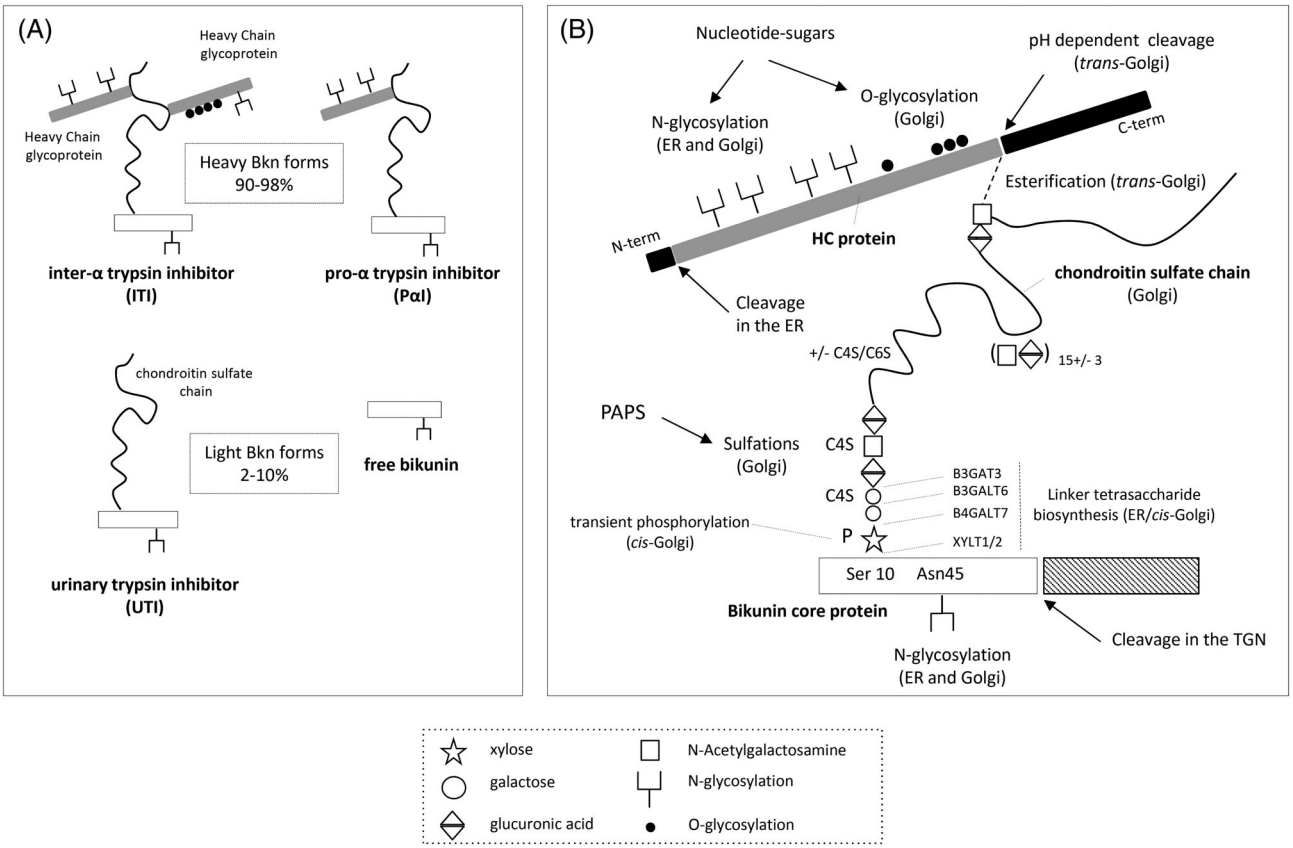

FIGURE 1 Schematic summary of known bikunin (Bkn) isoforms posttranslational modifications (PTMs). **A**, Structure details of the circulating Bkn isoforms consisting of inter-α-trypsin inhibitor (ITI) and pro-α-trypsin inhibitor (PαI) (the major fraction), and urinary trypsin inhibitor (UTI) (bikunin linked to chondroitin sulfate chain [Bkn-CS]) and free Bkn (the minor fraction). **B**, Ser10 of the core protein is xylosylated in the endoplasmic reticulum (ER). The CS chain is initiated (GlcA-Gal-Gal-Xyl- tetrasaccharide) and elongated (GlcA-GalNAc- disaccharide repeats) in the Golgi. A transient phosphorylation of the Xyl is required for the second Gal linkage. Sulfation reactions in the Golgi require 3′-phosphoadenosine 5′-phosphosulfate (PAPS) as donor substrate. Esterification reactions between the heavy chain (HC) C-terminal Asp and one GalNAc of the CS chain occur in the *trans*-Golgi in association with the pH-dependent C-terminal autocatalytic cleavage of the HC proteins precursors. Very unusually, the N-terminal cleavage of the HC precursors occurs in the ER. *N*-glycosylation is initiated in the ER and continues in the Golgi. Mucin core1 *O*-glycosylation occurs only in the Golgi. The glycosyltransferases involved in the biosynthesis of *N*-glycans, *O*-glycans, and of the CS chain need nucleotide-sugars as donor substrates. The C-terminal cleavage of the core protein precursor occurs in the *trans*-Golgi network just before its secretion into the blood. C4S/C6S: sulfated C-4/C-6; TGN: *trans*-Golgi network

2 | MATERIALS AND METHODS

2.1 | Serum/plasma samples

All blood samples were collected in agreement with the ethical policy of each institution. It should be underlined that, for some samples we tested, we could not determine whether they were anticoagulated (plasma) or not (sera).

Control samples originated from CDG-negative pediatric patients (n = 16), obese adults waiting for bariatric surgery (n = 11; cohort of Louis-Mourier Hospital; Dr S. Ledoux) and adult individuals with various pathologies (n = 9) including liver diseases (n = 6) such as cirrhosis, fibrosis and hepatitis (Antoine Béclère Hospital). Samples from patients with morbid obesity and liver diseases were tested since these conditions were shown to be frequently associated with secondary glycosylation abnormalities. Serum/plasma samples from CDG patients, mainly detected and diagnosed in our laboratory, were selected as follows: 3 ATP6V0A2-CDG (ATP6V0A2#1 to ATP6V0A2#3), 3 CCDC115-CDG (CCDC115#1 to CCDC115#3), 2 ATP6AP1-CDG (ATP6AP1#1 and ATP6AP1#2), 2 TMEM165-CDG (TMEM165#1 and TMEM165#2) (from Dr F. Foulquier and Prof J. Jaeken), 5 COG-CDG (2 COG5--CDG: COG5#1 and COG5#2; 3 COG7-CDG: COG7#1 to COG7#3), one SLC35A2-CDG and one SLC35A3-CDG. Clinical data and identified gene variants of studied CDG patients are available in Supp. File 1.

Samples from patients with linkeropathy (Prof V. Cormier-Daire) originated from individuals deficient in B4GALT7 (two unrelated individuals), B3GALT6 (one individual), and B3GAT3 (one individual). Detailed gene

variants were as follows: *B4GALT7* (a) and *B4GALT7* (b): ex.5 c.808C > T p.Arg270Cys (same missense mutation); *B3GALT6*: ex.1 c.353del p.Asp118Alafs*160-ex.1 c.653A > T p.Tyr218Phe (missense mutation); *B3GAT3*: ex3. c.461C > T p.Thr139Met (missense mutation). Brief clinical data of studied linkeropathy patients are available in Supp. File 1.

2.2 | Albumin level measurement

Albumin (Alb) levels of all the samples were determined (VISTA 1500 from Siemens) and measured values were used as loading controls in order to check for possible quantitative discrepancies with presented Western-blot visual results.

2.3 | Western-blot of Bkn isoforms

For the Western-blot analysis, sera/plasma were either diluted 1/10 (for UTI and free Bkn) or 1/250 (for ITI and PαI) in water. These dilutions were considered as "optimal" based on our previous work[2] and on the prior analysis of various sera and corresponding plasma sequentially diluted within 1/10 to 1/4000 (Supp. Figure S1).

Total of 20 μL of the diluted sera/plasma was mixed with Laemmli sample buffer (4X concentrate) and heated at 100°C for 10 minutes. Polyacrylamide gel electrophoresis, with 10 μL of treated sample loaded per well for all patients, was conducted using Nu-PAGE 4% to 12% bis-tris gels (ThermoFisher; cat. # NP0336BOX), as recommended by the manufacturer. After transfer to nitrocellulose (70 minutes, 100 V), heavy (ITI and PαI) and light Bkn isoforms (UTI and free Bkn) were detected after incubation with rabbit anti-Bikunin (CP6) polyclonal antibody (Merck-Millipore, cat. # ABT1346; 1/5000 in TTBS-5% milk for 90 minutes). Concerning this commercial primary antibody, the manufacturer indicates that "human ITI, PαI, bikunin-CS (UTI), and bikunin were specifically detected using a representative lot of this antibody." HRP-linked anti-rabbit secondary antibodies (Cell Signaling Technologies; cat. # 7074) were used (1/5000 in TTBS-5% milk). Finally, ECL revelation was conducted using Clarity Western ECL Substrate (cat. # 170-5060) and ChemiDoc XRS+ camera from Bio-Rad. Signal measurements (after background subtraction) of Bkn isoforms and relative quantitation of ITI and PαI were performed using ImageJ software.

2.4 | Two-dimensional electrophoresis

2-DE of proteins from 5 μL of crude serum/plasma from patients with linkeropathy was conducted using ZOOM strip pH 4 to 7 (ThermoFisher; cat. # ZM0012) for the first dimension and 4% to 12% Nu-PAGE bis-tris gel (ThermoFisher; cat. # NP0330BOX) for the second dimension, as recommended by the manufacturer. After 2-DE, separated proteins were transferred (90 minutes, 100 V) to nitrocellulose sheets and the abnormal serum Bkn light forms were detected using Clarity Western ECL Substrate (Bio-Rad) and ECL HyperFilm from GE Healthcare (cat. # 28906843). Film-based revelation was here preferred because of its higher sensitivity toward the detection of abnormal Bkn light forms compared with our camera system.

For the study of the phosphorylation state of Bkn abnormal light forms, samples were treated with commercial alkaline phosphatase (ALP) as recommended by the manufacturer (Roche; cat. # 10713023001). Briefly, samples (8 μL) were treated overnight at 37°C with a mixture of ALP (1 μL) and ALP buffer (1 μL) and were then analyzed by 2-DE as described above.

3 | RESULTS

3.1 | Western-blot of bikunin isoforms in CDG and linkeropathies

Western-blot patterns of all Bkn isoforms from one representative control, various type 2 CDG (CDG-II), and linkeropathy samples are shown in Figure 2A (free Bkn and UTI) and Figure 2B (PαI and ITI). As previously described,[2] the Bkn patterns from the 10-fold diluted control serum (Figure 2A) presented a small band at 25 kDa consistent with free Bkn and a ~35 kDa marked and large band corresponding to UTI, that is, Bkn linked to the variable-sized CS chain (Bkn-CS). Using a 250-fold diluted serum, the heavy Bkn isoforms could be seen (Figure 2B) as two bands at 125 and 225 kDa corresponding, respectively, to PαI (Bkn-CS-HC) and ITI (Bkn-CS-2HC). Also, ITI levels in controls (Figure 2B; Supp. Figure S2) were systematically higher than those of PαI.

In CDG with Golgi proton pump defects (ATP6V0A2-CDG, CCDC115-CDG and ATP6AP1-CDG), the free Bkn corresponding band at 25 kDa was either absent (2/3 ATP6V0A2-CDG; 3/3 CCDC115-CDG; 1/2 ATP6AP1-CDG) or found in small amounts (other cases) compared to control. The apparently abnormal and large free Bkn band observed in one ATP6V0A2-CDG patient (Figure 2A, arrowhead) was likely due to an important level of free Bkn leading to signal saturation. The UTI protein band was similar to that of the control in 2/3 ATP6V0A2-CDG cases and shared a mildly higher molecular weight (MW) in other proton pump-related CDG cases (Figure 2A). However, the corresponding MW

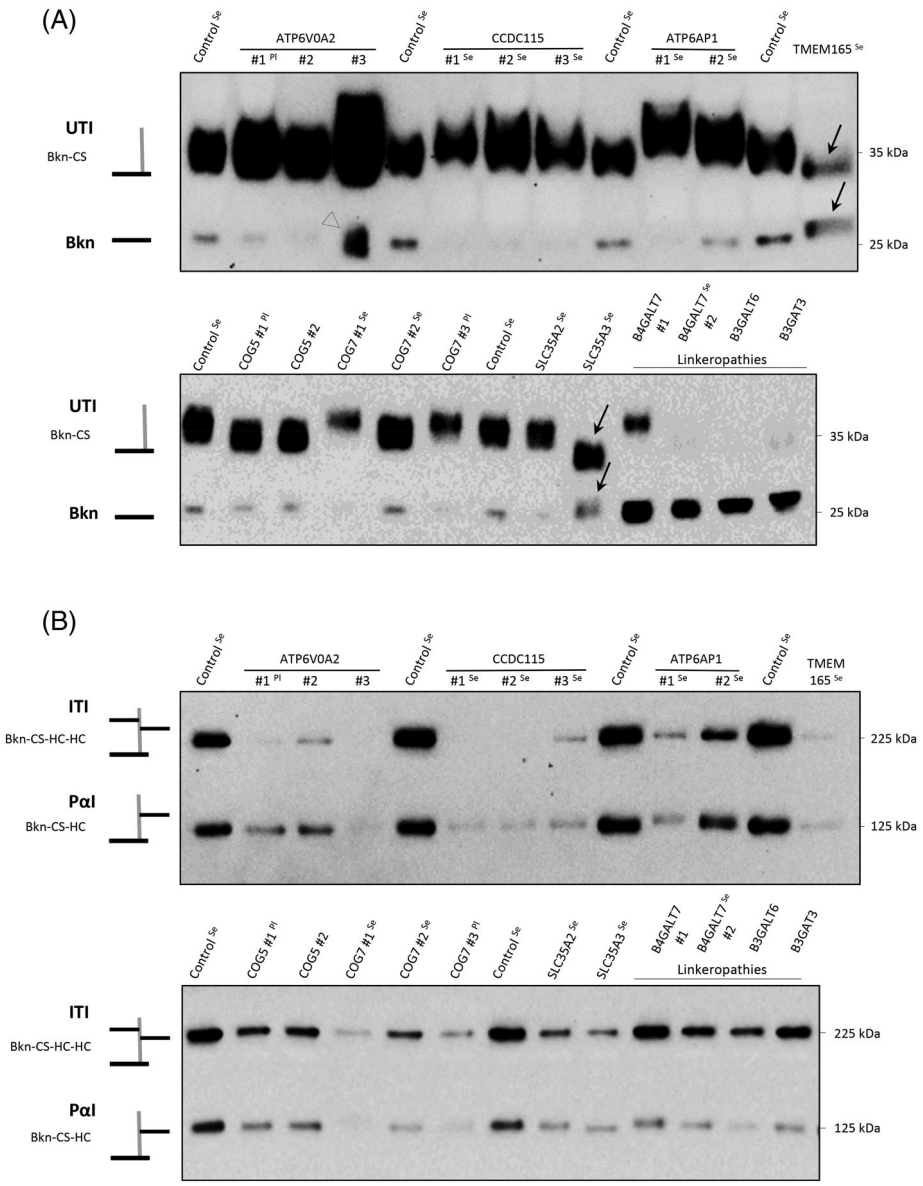

FIGURE 2 Western-blot profiles of all bikunin (Bkn) isoforms in various congenital disorder(s) of glycosylation type 2 (CDG-II) and linkeropathies. Western-blot of Bkn light forms, **A**, and heavy forms, **B**, from CDG with defects in: protons pump deficiencies (ATP6V0A2-CDG; CCDC115-CDG; ATP6AP1-CDG), Mn2+ homeostasis (TMEM165-CDG), retrograde Golgi trafficking (conserved oligomeric Golgi complex [COG]-CDG), sugar transporters (SLC35A2-CDG and SLC35A3-CDG) and in linkeropathies. Se, serum; Pl, plasma. Arrows indicate the major observed abnormalities

values remain included within normal values we determined previously.[2] Concerning the heavy forms, the overall signal levels of ITI and PαI were dramatically decreased compared to control with exception of one ATP6AP1-CDG sample showing a discrete reduced signal. To exclude any visual discrepancies related to possible major protein level differences between wells (under the same volume), ITI and PαI signals of each analyzed sample were adjusted with corresponding albumin level value (Suppl. Table S1). Thus, all observed major signal decreases we described were fully corroborated. Moreover, these decreases were systematically associated with an inversion of the ITI/PαI ratio in comparison with various control groups consisting of 16 non-CDG pediatric patients, 11 obese adults, and 6 individuals with liver diseases (Figure 2B; Supp. Figures S2 and S5).

Since we did not know whether some of the samples we tested were plasma or serum, it is important to note that the impact of the coagulation was tested to avoid potential discrepancies in our conclusions. Indeed, a prior Western-blot analysis was undertaken (Suppl. Figure S1) showing that the signal levels of ITI, PαI, UTI, and free Bkn appeared mildly decreased in serum compared to plasma. Thus, given that the control sample in Figure 2 is a serum, it is very likely that the marked decreased signal levels we describe are not related to the potential plasma nature of the related samples.

In the TMEM165-CDG patient, a genetic defect affecting Golgi Mn^{2+} homeostasis, the overall serum Bkn isoforms signal levels were dramatically decreased (Figure 2) and an abnormal ~27 kDa band associated with an abnormally low UTI MW could also be noticed (Figure 2A). Furthermore, the ITI/PαI ratio was also altered (Figure 2B; Supp. Figure S2). An additional TMEM165-CDG serum sample was analyzed during the redaction of this article, showing similar abnormal Bkn profiles (Supp. Figure S3).

In COG-CDG, the free Bkn band appeared similar to that of the control in 2/2 COG5-CDG cases and in 1/3 COG7-CDG, while it was barely detectable in the two remaining COG7-CDG cases (Figure 2A). For ITI and PαI, we observed overall decreased signal levels compared to the control, with particularly low signal observed for 2/3 COG7-CDG cases. In addition, in all COG-CDG cases, the ITIform was predominant with percentages ranging from 74% to 98% (Figure 2B; Supp. Figure S4).

In the SLC35A2-CDG (UDP-Gal transporter deficiency) studied serum, Bkn light forms did not show any abnormality (Figure 2A). Furthermore, the ITI/PαI ratio appeared similar to that of controls in association with a serum level decrease of these two heavy Bkn forms (Figure 2B; Supp. Figure S4). In the serum from the SLC35A3-CDG (UDP-GlcNAc transporter deficiency) individual, an abnormal ∼27 kDa band associated with an abnormally low UTI (Bkn-CS) MW could be evidenced (Figure 2A) with an ITI/PαI pattern similar to that of SLC35A2-CDG (Figure 2B; Supp. Figure S4). Finally, in linkeropathy samples, we corroborated the previously reported defects, consisting of abnormal light forms of ∼27 kDa and undetectable UTI in 3/4 cases (Figure 2A). Interestingly, the two samples from the patients sharing the same *B4GALT7* variant showed a marked discrepancy in the observed UTI signal. Finally, concerning ITI/PαI levels and ratios, no clear associated defect was noted (Figure 2B; Supp. Figure S4).

In summary, concerning Bkn light forms, marked abnormalities were observed for TMEM165-CDG, SLC35A3-CDG, and all tested linkeropathy individuals. Regarding the two heavy Bkn forms, dramatically decreased signals coupled to inverted ratios were noted for nearly all (except ATP6AP1#2) of the V-ATPase defects and for the two TMEM165-CDG individuals. For 2/3 COG7-CDG individuals, a decreased ITI/PαI signal was observed without associated inverted ratio. Finally, no evident abnormality was found in the heavy Bkn forms of linkeropathy patients.

3.1.1 | 2-DE of abnormal bikunin light forms in linkeropathies

Abnormal Bkn light forms in samples from patients with linkeropathy (Figure 3A) were analyzed by 2-DE. As shown in Figure 3B, while the samples from the two patients with B4GALT7 deficiency (ie, the enzyme involved in the first Gal linkage to -Xyl-O-Bkn) showed very similar patterns with up to three protein spots, those from the patients with a deficiency in the two subsequent enzymes were clearly different from the first ones and from each other. More precisely, the migration of the observed abnormal major Bkn light forms increasingly shifted toward the anode, according to the defective enzymes, that is, B4GALT7, B3GALT6, or B3GAT3, respectively. In addition, the 2-DE analysis of a mixture of samples (in ratios 1:1:1) from B4GALT7-, B3GALT6-, and B3GAT3-deficient patients corroborated the observed differences of charge and further exhibited increasing MW differences.

In order to evaluate the phosphorylation state of the abnormal Bkn light forms in linkeropathy patients, samples were first treated with ALP prior 2-DE analysis (Figure 3C). For the ALP-treated serum from B4GALT7-deficient patient, no difference in the migration was observed. In contrast, for ALP-treated samples from B3GALT6- and B3GAT3-deficient patients, we observed a cathodic shift of the major Bkn spots consistent with the ALP-mediated loss of a negatively charged phosphate group.

4 | DISCUSSION

In patients with Golgi protons pump defects that is, ATP6V0A2-CDG, CCDC115-CDG, and ATP6AP1-CDG, the serum/plasma levels of the Bkn core protein were decreased or undetectable in all except one case of ATP6V0A2-CDG. This result does not seem to be specific of the potential pH defect as similar Bkn patterns were also seen in other investigated controls (eg, in Suppl. Figure S1). It is likely that Golgi pH disturbances have no effects on the biosynthesis and/or secretion of the free Bkn core protein. Similarly, no major quantitative or qualitative defects were observed for UTI (Bkn-CS). Thus, this apparent lack of major CS GAG biosynthesis defects in Golgi protons pump-related CDG is in sharp contrast with abnormal *N*- and *O*-glycosylation reported elsewhere.[16-18] Concerning heavy Bkn isoforms, an inversion of the ITI/PαI ratio was observed in these three CDG subtypes compared to control groups. Moreover, the circulating levels of these two heavy forms were dramatically decreased. This has been already observed in individuals with severe acute infection,[19] which was not the case in our investigated patients. Furthermore, these decreases are specific for Bkn isoforms as albumin measurements in the analyzed samples allowed to exclude associated major protein level decreases compared to control.

ATP6V0A2-CDG, CCDC115-CDG, and ATP6AP1-CDG are genetic deficiencies affecting the V-ATPase protons pump, which plays pivotal roles not only in the luminal *trans*-Golgi acidification, but also in vesicular trafficking, fusion of vesicles and protein sorting.[20,21] While ATP6V0A2 is a subunit of the proton translocator

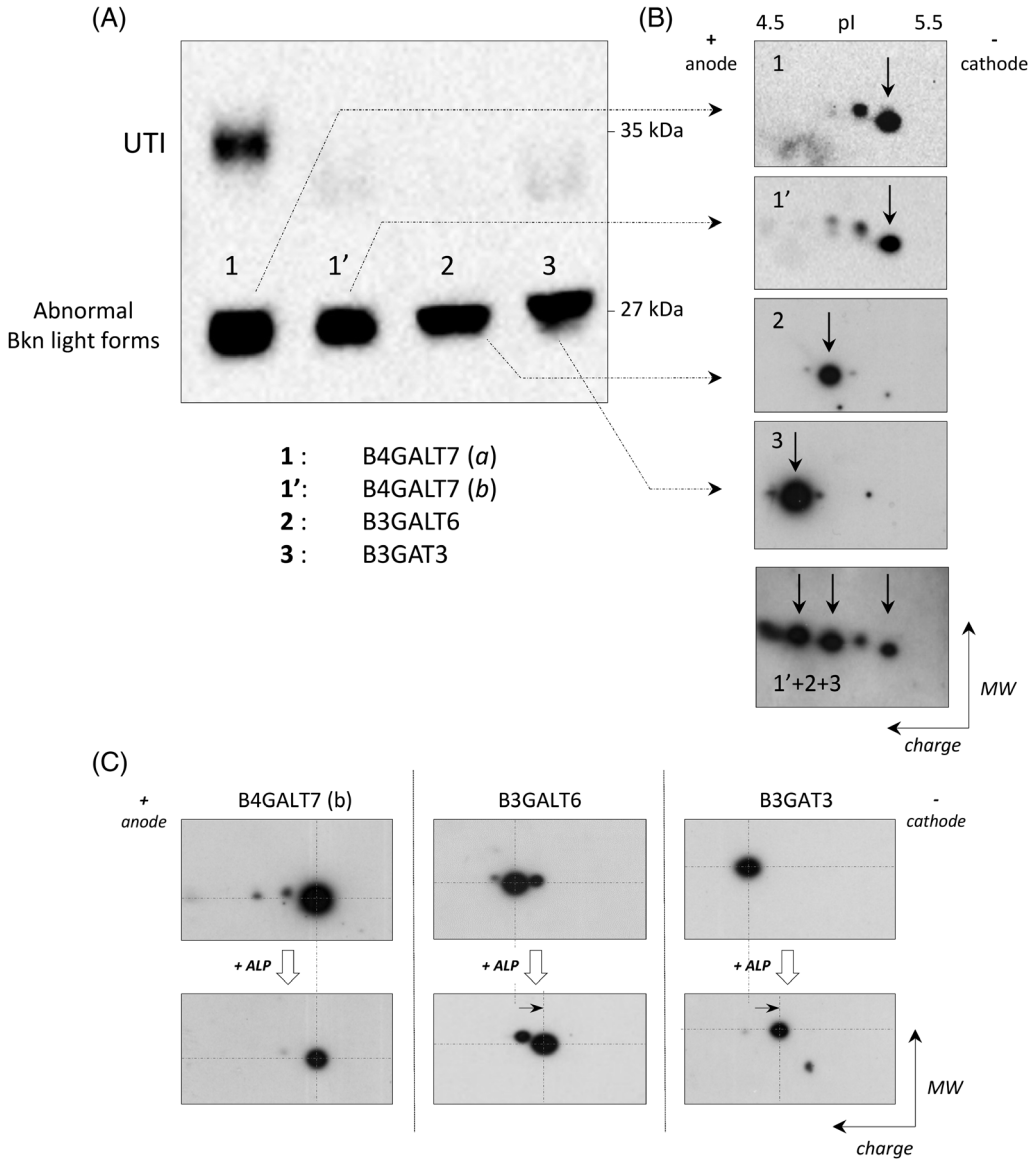

FIGURE 3 Serum/plasma bikunin electrophoretic profiles in linkeropathies. **A**, Western-blot patterns of abnormal light Bkn forms (~25-27 kDa) in samples from B4GALT7 (1 and 1′), B3GALT6 (2), and B3GAT3 (3) deficient patients. **B**, Corresponding two-dimensional electrophoresis (2-DE) patterns showing an anodic shift of the major Bkn spots (arrows). The 2-DE profile of a mixture (in ratios 1:1:1) of B4GALT7-, B3GALT6-, and B3GAT3-deficient patients' samples (1′ + 2 + 3) corroborated the charge differences and evidenced molecular weight (MW) differences. pI: isoelectric point. **C**, 2-DE patterns of abnormal Bkn light forms in B4GALT7-, B3GALT6-, and B3GAT3-deficient patients' samples, before (up) and after (below) alkaline phosphatase (ALP) treatment. Small horizontal arrows indicate the cathodic shift observed for the major spot

V0 domain of the V-ATPase,[16] CCDC115 and ATP6AP1 are assembly factor and accessory subunit of this complex, respectively.[17,22] Thus, as expected, it would appear that the impaired acidification of the *trans*-Golgi associated with these CDG does not affect the Bkn CS chain biosynthesis that essentially takes place in early Golgi compartments. Conversely, the observed ITI/PαI ratio inversion and overall decreased levels suggest that this *trans*-Golgi acidification defect might impair the pH-dependent protein cleavage of HCs precursors and disturb their ester linkage to the CS chain. Since it has been shown that an increased pH in the *trans*-Golgi could lead to *N*- and *O*-glycosyltransferases mislocalization, inactivation, and interaction defects,[23,24] similar consequences on putative ester transferases responsible for the linkages of HCs to the CS chain could also be evoked and will need to be further addressed. In addition, the vesicular trafficking defects related to V-ATPase deficiencies could

also contribute to the mislocalization of the ester transferases and to a decreased protein secretion.

TMEM165 is a Ca^{2+}-Mn^{2+}/H^+ Golgi antiporter playing a pivotal role in the Golgi luminal pH maintenance and in the level of Mn^{2+} cations that are important cofactors of specific Golgi-resident glycosylation enzymes.[25,26] In the two presented TMEM165-CDG cases, we report marked defects in the light Bkn forms patterns as well as in ITI/PαI signal levels and ratios (Figure 2). For light Bkn forms, the observed impairments suggest combined defects in the initiation and in the elongation of the CS chain. They could be related to overall enzymatic defects linked to Golgi Mn^{2+} deficiency and strongly fit with the major skeletal phenotype of the investigated patients.[27] In this regard, TMEM165-CDG interestingly appears as a genetic disease affecting *N*-glycosylation, *O*-glycosylation, glycolipids, and the CS biosynthesis. Concerning the heavy Bkn forms (ITI and PαI) in TMEM165-CDG, the observed abnormalities are highly comparable to those found in V-ATPase deficiencies. As regarding the similarity of the glycosylation defects between these CDG subtypes,[25] our results are consistent with potential Golgi pH-related PTM alterations, not only affecting the *N*- and *O*-glycosylation, but also the CS-HC esterification. The involvement of the Mn^{2+} deficiency in the impairment of esterification and protein sorting could also be suspected and will need further testing.

The multisubunit COG complex is a molecular tethering factor mainly involved in the retrograde trafficking from the *cis*-Golgi to the ER and its impairment was shown to affect *N*- and mucin type *O*-glycosylation mainly through the mislocalization of the related enzymes.[28] In COG-CDG samples, the observed absence of defects in the UTI biosynthesis (Figure 2) suggests COG is not involved in the subcellular localization of the enzymes involved in the CS chain synthesis. Although unexpected, this observation is supported by a recently published "organelle zones" theory, which differentiates in the Golgi a "proteoglycan zone" from a "mucin zone" with variable responses to different stresses.[29] Concerning the observed ITI and PαI decreased levels, they could be explained by HCs glycosylation defects that would decrease the secretion or increase the degradation of heavy Bkn isoforms.

SLC35A2 protein mainly corresponds to UDP-galactose (UDP-Gal) Golgi transporter.[30] Since Gal residue is a key monosaccharide for N-glycosylation, SLC35A2 deficiency was expected to be associated with abnormal transferrin (Trf) patterns. However, it has been recently shown in two distinct cohorts that the screening of SLC35A2-CDG could be very challenging with only 35% to 60% of samples sharing Trf N-glycosylation abnormalities.[31,32] We previously showed that the SLC35A2-CDG case used in this study harbored markedly abnormal CDG-II Trf pattern.[33] In contrast, the observed normal light Bkn forms pattern suggests a normal tetrasaccharide linker synthesis despite the presence of two Gal residues in this structure. Thus, this observation could be linked, in this case, to the preferential use of UDP-Gal toward the GAG biosynthesis rather than N-glycosylation. Nevertheless, it could be possible that other causal *SLC35A2* gene variants (notably those associated with a skeletal phenotype) could lead to an abnormal light Bkn forms pattern, with potential screening/diagnosis interest. Concerning heavy Bkn forms in the SLC35A2-CDG case, the observed decreases of heavy Bkn isoforms in absence of an obvious Golgi homeostasis disturbance could be related to abnormal protein elimination and/or sorting associated with abnormal HCs glycosylation. [Correction added on 12 August 2021, after print and online publication: The two preceding sentences were previously missing and has been added in this version.]

SLC35A3-CDG is an inherited deficiency in UDP-*N*-acetylglucosamine (UDP-GlcNAc) Golgi transporter typically associated with *N*-glycosylation abnormalities in agreement with the involvement of GlcNAc moieties in the *N*-glycan core structure.[30,33] Since GlcNAc is lacking in the CS chains, the abnormal Bkn light form and the abnormally low UTI MW (Figure 2) are surprising in the SLC35A3-CDG. Nevertheless, they could result from major interaction defects with other Golgi sugar transporters involved in the CS biosynthesis, including SLC35A2.[34] Moreover, this alteration in the pattern of serum Bkn light forms suggests overall CS defects in line with the skeletal abnormalities observed in our patient (showing major long bones growth retardation) as well as in other cases described elsewhere.[35,36]

Inherited defects in the enzymes involved in the stepwise synthesis of the common GAG tetrasaccharide linker, that is, xylosyltransferases (XYLT1 or XYLT2), galactosyltransferases (B4GALT7 and B3GALT6), and glucuronyltransferase (B3GAT3), correspond to linkeropathies.[37] In this work, we corroborated previously described high levels of abnormal Bkn light forms in B4GALT7, B3GALT6, and B3GAT3 deficiencies (Figure 2). Furthermore, we showed a quasi-absence of circulating normal UTI in 3/4 samples coupled with unexpectedly normal ITI and PαI signal levels and ratios. Hence, it would appear that missense mutations found in the four cases studied would allow residual UTI biosynthesis, the latter being sufficient for normal HC ester linkages in the *trans*-Golgi. Moreover, it is likely that once mostly used for ITI and/or PαI synthesis, the remaining intracellular stock of normal UTI could be very low in 3/4 patients, finally leading to its severely reduced blood secretion. Concerning the different UTI levels that we observed in the two patients sharing the same *B4GALT7* variant, they could be linked to distinct

UTI requirements toward the formation of ITI and PαI according to the patient's condition at the sampling time.

By coupling charge- and MW-based separation (2-DE), we showed that the abnormal Bkn light forms found in linkeropathies were clearly different according to the mutated gene (Figure 3). Since it has been shown that the transient 2-O-phosphorylation of the xylose is required for the B3GALT6-catalyzed linkage of the second galactose,[38,39] the anodic shift observed between the major spots detected in samples from B4GALT7- and B3GALT6-deficient patients could be consistent with the presence of Xyl-O-Bkn in the first case, and Gal-Xyl(2-O-phoshate)-O-Bkn in the second case. Indeed, the cathodic shift induced by phosphatase treatment corroborated the presence of a phosphate in the Bkn linkage region from the B3GALT6-deficient patient, contrary to the B4GALT7-deficient case. In the ALP-treated sample from the B3GAT3-deficient patient, a cathodic shift was also observed. Thus, since the second Gal residue of the UTI tetrasaccharide linker has been shown to be systematically sulfated,[3,40] the observed shift between B3GALT6- and B3GAT3-deficient patients could correspond to the presence of Gal(4-C-sulfate)-Gal-Xyl(2-O-phosphate)-O-Bkn in the B3GAT3-deficient patient's sample.

Finally, it is likely that the other observed minor spots are linked to other modifications such as *N*-glycosylation,[7] sialylation of the first gal residue, xylose fucosylation[41] or a recently reported non-canonical CS linkage region trisaccharide (GlcA-Gal-Xyl-O).[42]

Although limited to a small number of patients with linkeropathy, our results are consistent with the current knowledge about the early steps of the Bkn-linked CS chain synthesis and highlight the existence of 2-DE signature patterns.

When assessed in their clinical context and summarized in a decisional tree (Figure 4), our results first indicate that the heavy Bkn isoforms electrophoretic profile could be a convenient additional tool in the CDG-II diagnosis pathway, complementing the second-line MS-based glycomic studies and apolipoprotein C-III (apoC-III) analysis (Figure 4A). Second, our findings also reveal that the light Bkn isoforms pattern could be of interest for the screening of TMEM165-CDG, SLC35A3-CDG, and patients with linkeropathies, with probable signature 2-DE patterns for the latter ones (Figure 4B).

5 | CONCLUSIONS

Bikunin isoforms are multifaceted circulating proteoglycans whose the follow-up of the diverse PTMs can be used as biomarkers for the screening and diagnosis of various genetic diseases, including linkeropathies and inherited defects of Golgi ion homeostasis. Further work will now be important to enlarge the analysis of Bkn isoforms to additional CDG/linkeropathy samples. In this way, particular interest will be paid toward (a) other CDG with Golgi homeostasis defects associated with

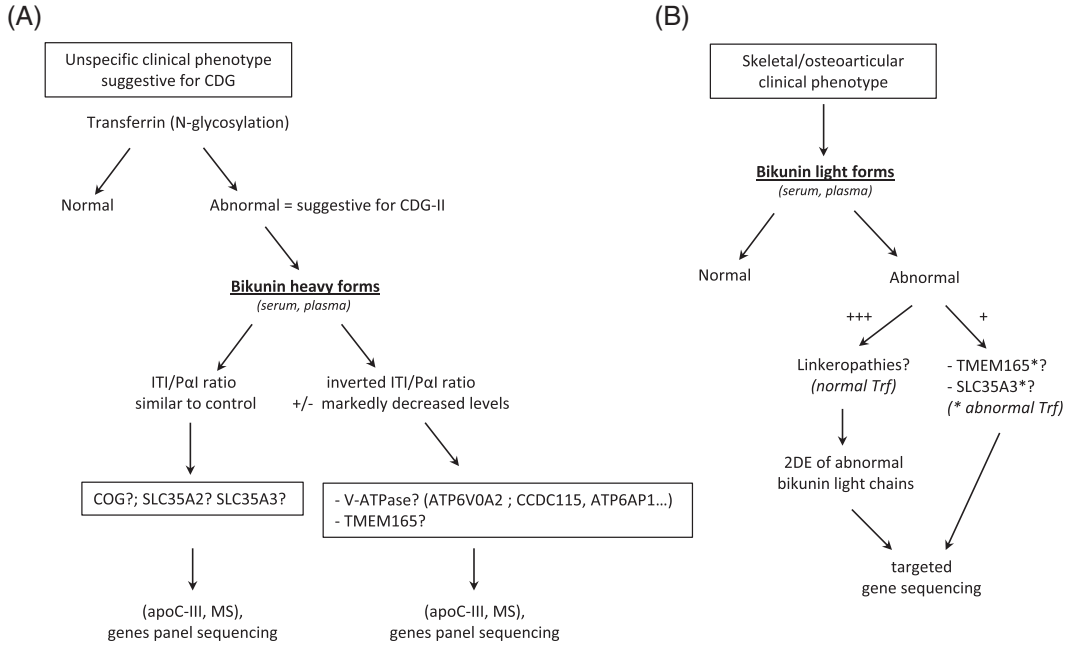

FIGURE 4 Suggestion of a decisional tree summarizing the main diagnostic orientations given by our bikunin isoforms analysis. **A**, In the diagnosis pathway of congenital disorder(s) of glycosylation type 2 (CDG-II). **B**, In the diagnosis pathway of TMEM165-CDG, SLC35A3-CDG and linkeropathies. ApoC-III, apolipoprotein C-III; MS, mass spectrometry

skeletal phenotypes (eg, SLC10A7-CDG, SLC39A8-CDG, COG4-CDG, etc.) and (b) inherited defects in the elongation of the CS chain (eg, CS synthase deficiencies). Finally, we will also evaluate the potentials of the Bkn isoforms' patterns in the diagnosis of the GAG sulfation defects.

ACKNOWLEDGMENTS

This work was supported by grant ANR-15RAR3-0004-06 under the frame of E-RARE-3, the ERA-Net for Research on Rare Diseases; it was also supported by the European Union's Horizon 2020 Research and Innovation Program under the ERA-NET cofund action No. 643578. The authors confirm independence from the sponsors; the content of the article has not been influenced by the sponsors.

CONFLICT OF INTEREST

The authors declare no conflict of interest.

AUTHOR CONTRIBUTIONS

Walid Haouari: PhD student. Performed the majority of the experiments; wrote the article with Arnaud Bruneel. **Johanne Dubail**: Importantly involved in linkeropathy patients diagnosis and samples management. Critical reading of the manuscript. **Samra Lounis-Ouaras**: Performed the experiments relative to controls with liver diseases. Critical reading of the manuscript. **Pierre Prada**: Performed some important 2-DE experiments. **Rizk Bennani**: Performed some very important Western-blotting experiments. **Charles Roseau**: Importantly involved in the development of the Western-blot detection of bikunin isoforms. **Céline Huber**: Molecular diagnosis and clinical management of the linkeropathy patients. **Alexandra Afenjar**: Molecular diagnosis and clinical management of the patient COG5#2. **Estelle Colin**: Molecular diagnosis and clinical management of the patients COG7#1 and COG7#2. **Sandrine Vuillaumier-Barrot**: Molecular diagnosis of patients ATP6V0A2#1, ATP6V0A2#2, CCDC115#1 to #3 and SLC35A2. **Nathalie Seta**: Critical reading of the manuscript; supervision of the work with **Arnaud Bruneel**. **François Foulquier**: Critical reading of the manuscript and notably the part related to TMEM165-CDG. **Christian Poüs**: Team leader of UMR1193. Critical reading of the paper; supervision of the work with Arnaud Bruneel. **Valérie Cormier-Daireand**: Leader of UMR1163. Significantly contributed to the initiation of this work. Critical reading of the manuscript; recruitment of linkeropathy patients. **Arnaud Bruneel**: Wrote the manuscript with Walid Haouari. Supervision and direction of all the experiments and collaborative works.

INFORMED CONSENT

All procedures followed were in accordance with the ethical standards of the responsible committee on human experimentation (institutional and national) and with the Helsinki Declaration of 1975, as revised in 2000. Informed consent was obtained from all patients for being included in the study.

ORCID

Arnaud Bruneel https://orcid.org/0000-0001-8411-3309

REFERENCES

1. Salier JP, Rouet P, Raguenez G, Daveau M. The inter-alpha-inhibitor family: from structure to regulation. *Biochem J*. 1996; 315(Pt 1):1-9.
2. Bruneel A, Dubail J, Roseau C, et al. Serum bikunin is a biomarker of linkeropathies. *Clin Chim Acta*. 2018;485:178-180.
3. Ly M, Leach FE, Laremore TN, Toida T, Amster IJ, Linhardt RJ. The proteoglycan bikunin has a defined sequence. *Nat Chem Biol*. 2011;7(11):827-833.
4. Paganini C, Costantini R, Superti-Furga A, Rossi A. Bone and connective tissue disorders caused by defects in glycosaminoglycan biosynthesis: a panoramic view. *FEBS J*. 2019;286(15):3008-3032.
5. Thuveson M, Fries E. The low pH in trans-Golgi triggers autocatalytic cleavage of pre-alpha-inhibitor heavy chain precursor. *J Biol Chem*. 2000;275(40):30996-31000.
6. Flahaut C, Capon C, Balduyck M, Ricart G, Sautiere P, Mizon J. Glycosylation pattern of human inter-alpha-inhibitor heavy chains. *Biochem J*. 1998;333(Pt 3):749-756.
7. Enghild JJ, Thøgersen IB, Cheng F, Fransson LA, Roepstorff P, Rahbek-Nielsen H. Organization of the inter-alpha-inhibitor heavy chains on the chondroitin sulfate originating from Ser (10) of bikunin: posttranslational modification of IalphaI-derived bikunin. *Biochemistry*. 1999;38(36):11804-11813.
8. Thuveson M, Fries E. Intracellular proteolytic processing of the heavy chain of rat pre-alpha-inhibitor. The COOH-terminal propeptide is required for coupling to bikunin. *J Biol Chem*. 1999;274(10):6741-6746.
9. Héron A, Bourguignon J, Callé A, et al. Post-translational processing of the inter-alpha-trypsin inhibitor in the human hepatoma HepG2 cell line. *Biochem J*. 1994;302(Pt 2):573-580.
10. Zhu L, Zhuo L, Watanabe H, Kimata K. Equivalent involvement of inter-alpha-trypsin inhibitor heavy chain isoforms in forming covalent complexes with hyaluronan. *Connect Tissue Res*. 2008;49(1):48-55.
11. Zhuo L, Hascall VC, Kimata K. Inter-alpha-trypsin inhibitor, a covalent protein-glycosaminoglycan-protein complex. *J Biol Chem*. 2004;279(37):38079-38082.
12. Pratt CW, Pizzo SV. Mechanism of action of inter-alpha-trypsin inhibitor. *Biochemistry*. 1987;26(10):2855-2863.
13. Yingsung W, Zhuo L, Mörgelin M, et al. Molecular heterogeneity of the SHAP-hyaluronan complex isolation and characterization of the complex in synovial fluid from patients with rheumatoid arthritis. *J Biol Chem*. 2003;278(35):32710-32718.
14. Kobayashi H, Suzuki M, Hirashima Y, Terao T. The protease inhibitor bikunin, a novel anti-metastatic agent. *J Biol Chem*. 2003;384(5):749-754.

15. Suzuki M, Kobayashi H, Kageyama S, Shibata K, Fujie M, Terao T. Excretion of bikunin and its fragments in the urine of patients with renal stones. *J Urol*. 2001;166(1):268-274.
16. Kornak U, Reynders E, Dimopoulou A, et al. Impaired glycosylation and cutis laxa caused by mutations in the vesicular H +-ATPase subunit ATP6V0A2. *Nat Genet*. 2008;40(1):32-34.
17. Jansen JC, Cirak S, van Scherpenzeel M, et al. CCDC115 deficiency causes a disorder of Golgi homeostasis with abnormal protein glycosylation. *Am J Hum Genet*. 2016;98(2):310-321.
18. Jansen EJR, Timal S, Ryan M, et al. ATP6AP1 deficiency causes an immunodeficiency with hepatopathy, cognitive impairment and abnormal protein glycosylation. *Nat Commun*. 2016;7:11600.
19. Daveau M, Rouet P, Scotte M, et al. Human inter-alpha-inhibitor family in inflammation: simultaneous synthesis of positive and negative acute-phase proteins. *Biochem J*. 1993;292 (Pt 2):485-492.
20. Forgac M. Vacuolar ATPases: rotary proton pumps in physiology and pathophysiology. *Nat Rev Mol Cell Biol*. 2007;8(11):917-929.
21. Cotter K, Stransky L, McGuire C, Forgac M. Recent insights into the structure, regulation, and function of the V-ATPases. *Trends Biochem Sci*. 2015;40(10):611-622.
22. Jansen EJR, Martens GJM. Novel insights into V-ATPase functioning: distinct roles for its accessory subunits ATP6AP1/Ac45 and ATP6AP2/(pro) renin receptor. *Curr Protein Pept Sci*. 2012;13(2):124-133.
23. Rivinoja A, Hassinen A, Kokkonen N, Kauppila A, Kellokumpu S. Elevated Golgi pH impairs terminal N-glycosylation by inducing mislocalization of Golgi glycosyltransferases. *J Cell Physiol*. 2009;220(1):144-154.
24. Hassinen A, Rivinoja A, Kauppila A, Kellokumpu S. Golgi N-glycosyltransferases form both homo- and heterodimeric enzyme complexes in live cells. *J Biol Chem*. 2010;285(23):17771-17777.
25. Dulary E, Potelle S, Legrand D, Foulquier F. TMEM165 deficiencies in congenital disorders of glycosylation type II (CDG-II): clues and evidences for roles of the protein in Golgi functions and ion homeostasis. *Tissue Cell*. 2017;49(2) Pt A:150-156.
26. Lebredonchel E, Houdou M, Potelle S, et al. Dissection of TMEM165 function in Golgi glycosylation and its Mn2+ sensitivity. *Biochimie*. 2019;165:123-130.
27. Zeevaert R, de Zegher F, Sturiale L, et al. Bone dysplasia as a key feature in three patients with a novel congenital disorder of glycosylation (CDG) type II due to a deep intronic splice mutation in TMEM165. *JIMD Rep*. 2013;8:145-152.
28. Blackburn JB, D'Souza Z, Lupashin VV. Maintaining order: COG complex controls Golgi trafficking, processing, and sorting. *FEBS Lett*. 2019;593(17):2466-2487.
29. Sasaki K, Yoshida H. Golgi stress response and organelle zones. *FEBS Lett*. 2019;593(17):2330-2340.
30. Hadley B, Maggioni A, Ashikov A, Day CJ, Haselhorst T, Tiralongo J. Structure and function of nucleotide sugar transporters: current progress. *Comput Struct Biotechnol J*. 2014;10(16):23-32.
31. Ng BG, Sosicka P, Agadi S, et al. SLC35A2-CDG: functional characterization, expanded molecular, clinical, and biochemical phenotypes of 30 unreported individuals. *Hum Mutat*. 2019;40(7):908-925.
32. Vals M-A, Ashikov A, Ilves P, et al. Clinical, neuroradiological, and biochemical features of SLC35A2-CDG patients. *J Inherit Metab Dis*. 2019;42(3):553-564.
33. Bruneel A, Cholet S, Drouin-Garraud V, et al. Complementarity of electrophoretic, mass spectrometric, and gene sequencing techniques for the diagnosis and characterization of congenital disorders of glycosylation. *Electrophoresis*. 2018;39(24):3123-3132.
34. Maszczak-Seneczko D, Sosicka P, Majkowski M, Olczak T, Olczak M. UDP-N-acetylglucosamine transporter and UDP-galactose transporter form heterologous complexes in the Golgi membrane. *FEBS Lett*. 2012;586(23):4082-4087.
35. Marini C, Hardies K, Pisano T, et al. Recessive mutations in SLC35A3 cause early onset epileptic encephalopathy with skeletal defects. *Am J Med Genet A*. 2017;173(4):1119-1123.
36. Edmondson AC, Bedoukian EC, Deardorff MA, et al. A human case of SLC35A3-related skeletal dysplasia. *Am J Med Genet A*. 2017;173(10):2758-2762.
37. Mizumoto S, Yamada S, Sugahara K. Mutations in biosynthetic enzymes for the protein linker region of chondroitin/-dermatan/heparan sulfate cause skeletal and skin dysplasias. *Biomed Res Int*. 2015;2015:861752.
38. Wen J, Xiao J, Rahdar M, et al. Xylose phosphorylation functions as a molecular switch to regulate proteoglycan biosynthesis. *Proc Natl Acad Sci U S A*. 2014;111(44):15723-15728.
39. Koike T, Izumikawa T, Sato B, Kitagawa H. Identification of phosphatase that dephosphorylates xylose in the glycosaminoglycan-protein linkage region of proteoglycans. *J Biol Chem*. 2014;289(10):6695-6708.
40. Yamada S, Oyama M, Yuki Y, Kato K, Sugahara K. The uniform galactose 4-sulfate structure in the carbohydrate-protein linkage region of human urinary trypsin inhibitor. *Eur J Biochem*. 1995;233:687-693.
41. Toledo AG, Nilsson J, Noborn F, Sihlbom C, Larson G. Positive mode LC-MS/MS analysis of chondroitin sulfate modified glycopeptides derived from light and heavy chains of the human inter-α-trypsin inhibitor complex. *Mol Cell Proteomics*. 2015;14(12):3118-3131.
42. Persson A, Nilsson J, Vorontsov E, Noborn F, Larson G. Identification of a non-canonical chondroitin sulfate linkage region trisaccharide. *Glycobiology*. 2019;29(5):366-371.

SUPPORTING INFORMATION

Additional supporting information may be found online in the Supporting Information section at the end of this article.

How to cite this article: Haouari W, Dubail J, Lounis-Ouaras S, et al. Serum bikunin isoforms in congenital disorders of glycosylation and linkeropathies. *J Inherit Metab Dis*. 2020;43:1349–1359. https://doi.org/10.1002/jimd.12291